Validation of a physics-based model for rolling element bearings with diagnosis purposes

Urko Leturiondo[1,2], Oscar Salgado[1], Diego Galar[2]

[1] IK4-Ikerlan Technology Research Centre, Control and Monitoring Area, P[o] J.M. Arizmendiarrieta, 2, 20500 Arrasate-Mondragón, uleturiondo@ikerlan.es , osalgado@ikerlan.es

[2] Luleå University of Technology, Division of Operation and Maintenance Engineering, 971 87 Luleå, diego.galar@ltu.se

Keywords: condition monitoring, model validation, vibration analysis, diagnosis, rolling element bearing

Abstract

The use of rolling element bearings is widely extended to many fields such as wind energy systems, transportation and machine tools, among others. This broad use makes their performance analysis an interesting field of research. There are techniques to determine the life of a bearing and the on-going failure, if any, under some assumptions with some values of reliability. However, the unfulfilment of those hypothesis or other effects that affect the standard operation of rolling element bearings (e.g. current leakage, overloading, corrosion, etc.) leads to a higher probability of the appearance of failure. The monitoring of the condition of rolling element bearings has two main goals, the diagnosis and the prognosis of the item. Indeed, diagnosis, i.e. damage detection, localization and identification, has a great interest on the knowledge of the state of rolling element bearings in order to prevent faulty situations that may cause risky or costly situations, identifying those adverse situations and trying to mitigate the undesired effects. Therefore, risky situations due to failures need additional knowledge about the dynamics of a system (rolling element bearings in this case) and physics-based models can be used in order to represent it. They have an interesting potential due to the fact that they are able to simulate situations that may arise in some damaged conditions that might be either difficult, costly or insecure to reproduce in a real system. However, there is a need to validate the physics-based models to assure that it follows the real response of the system. This work presents the validation process of a model already developed by the authors. Experimental tests have been done in a test rig and the vibration measurements taken from these tests have been used to validate the model. Damage on the surface of the outer race has been induced to one of the rolling element bearings of the test rig. Thus, frequency-domain and order-domain analysis have been performed and the experimental results have been compared to the results obtained from the simulations. Differences lower than 2.5 % have been found for a wide range of constant and variable speeds and, hence, the model is validated.

1. INTRODUCTION

The wide use of rolling element bearings (REBs) and their influence on the dynamics of the machines in which they are placed make them being one of the focus of maintainers. Although there are methods for the determination of their life, they are based in a number of hypothesis that are not fulfilled in real operation. That is why the monitoring of their condition has become a topic of great interest in the last decades. This technique, within a condition-based maintenance strategy, allow maintainers to increase the reliability, availability, maintainability and safety of the monitored machine, as well as extending its useful life, in such a way that maintenance tasks can be better planned and maintenance costs are reduced, despite the initial inversion needed to apply this approach.

In this condition monitoring framework, one of the goals is to perform the diagnosis process, that is, detect damage, identify the kind of damage and localise it. Carrying out this task properly gives

meaningful information to make maintenance decisions. Hence, there is a need to develop algorithms that help in this diagnosis task.

It is known that physics-based models are useful to obtain the behaviour of a system in different operating conditions as well as in different health states. As obtaining this information from the system itself might have some difficulties from the economic and/or safety point of view, physics-based models can be used to represent those situations. Nevertheless, there is a need for validation of these models to assure that their response is a true reflection of reality.

Many physics-based models for REBs that take into account the presence of damage in any of their parts can be found in literature [1]. Those models represent the dynamics of REBs under different hypothesis and taking into account different effects. For example, the bearing configuration considered when modelling, the number of degrees of freedom (DOF) and the kind of contacts are the major differences between those models. Yuan et al. [2] studied the motion of the shaft and the rolling elements of a single-row deep-groove ball bearing, assuming that both the shaft and the balls have 2 DOF each and that the contact forces are normal to the mating surfaces. In contrast, Niu et al. [3] introduced the tractive forces due to the lubrication and they also assumed the motion of the pedestal of a ball bearing by 2 translational DOF. More complex models for other kinds of REBs are also developed, such as the one proposed by Kogan et al. [4], who provided a model for a duplex angular-contact ball bearing as a combination of two angular-contact ball bearings. Another issue to be analysed is the nature of the damage, which can be modelled by several ways. Sopanen and Mikkola [5] considered the effect of defects introduced in the model as waviness produced by the manufacturing process and the effect of localised faults as the result of spalling. Nakhaeinejad and Bryant [6] modelled damage as a rectangular change of the geometry of the surface of the races as a localised fault. Other authors, such as Patel et al. [7], analysed the effect of having a single or two defects on the races.

Moreover, the validation itself is also performed by different techniques. Time-domain features can be used for evaluating the degradation state of a REB, as Sassi et al. [8] did for a ball bearing by the use of scalar indicators such as kurtosis, crest factor, shape factor and impulse factor, among others. Nevertheless, the most usual kind of validation is the one focused on the frequency-domain analysis by checking the characteristic fault frequencies. It is the case of Arslan and Aktür [9], who validated their 2 DOF model representing the motion of the inner ring of a REB by analysing the agreement of the characteristic frequencies when there is localised damage. The same approach is followed by Petersen et al. [10] who considered the existence of extended damage. Furthermore, the effect of other factors such as the shaft speed is analysed by Choudhury and Tandon [11].

In this paper the validation of a a model already developed by the authors is presented. It is a model that has as aim the modelling of any kind of REB using a multi-body approach. In this paper the model is validated for the case of a single-row deep-groove ball bearing. For that purpose, a number of tests in different operating conditions have been done by the use of a commercial test rig. For these tests, a healthy REB and a REB with localised damage in the outer ring have been used. The vibration of a REB is acquired, analysed and compared to the simulations results given by the aforementioned model to validate it by checking the characteristic fault frequencies.

This paper is structured as follows: Section 2 presents the model; the experimental equipment used and the tests are explained in Section 3; the validation of the model is presented in Section 4; and, finally, some concluding remarks are given in Section 5.

2. PHYSICS-BASED MODEL OF ROLLING ELEMENT BEARINGS

The model which is validated in this paper is the one proposed by Leturiondo et al. [12]. The authors presented a general approach for the physics-based modelling of REBs in different configurations, following a multi-body strategy. It is based in a set of models representing the characteristics of the parts that form a REB as well as the way in which the contacts between those parts are produced is defined.

In detail, the modelled parts are the rings, the rolling elements and the cage. They are considered to behave as rigid bodies with point mass, but elastic behaviour is considered in the zones where the

contact between the parts occurs. Thus, each part has 6 DOF to describe the translational and the rotational motion, defined by the linear position vector from the centre of a fixed reference system to the gravity centre of the body and the Euler parameters for the body-fixed reference system.

The dynamics of these parts are affected by the contact loads (force $\mathbf{f}_c$ and moment $\mathbf{m}_c$) between them. The contact force in the contact between the rolling elements and the rings is divided in two components: a component normal to the mating surface, $\mathbf{f}_N$, and a tangential component in the direction of rolling, $\mathbf{f}_T$. The former is calculated by the use of Hertz theory [13] and taking into account the dissipative effect as proposed by Flores et al. [14]. The expression for the normal force is

$$\mathbf{f}_N = \left[K_n \cdot \delta^n + \frac{3 \cdot K_n \cdot \left(1 - c_e^2\right)}{4 \cdot \dot{\delta}^{(-)}} \cdot \delta^n \cdot \dot{\delta} \right] \cdot \hat{\mathbf{n}} \tag{1}$$

where K_n is the contact stiffness, δ the contact deformation, n the load-deflection factor, which is equal to $3/2$ for ball bearings and to $10/9$ for any kind of roller bearings, c_e the restitution coefficient, $\dot{\delta}^{(-)}$ the initial normal impact velocity where the contact is produced and $\hat{\mathbf{n}}$ is the unitary normal vector. The calculation of the tangential force is based on the elastohydrodynamic lubrication (EHL) theory [15]

$$\mathbf{f}_T = \mu\left(\eta, \dot{\gamma}\right) \cdot |\mathbf{f}_N| \cdot \hat{\mathbf{t}} \tag{2}$$

where μ is the friction coefficient, η is the lubricant viscosity, $\dot{\gamma}$ is the strain rate and $\hat{\mathbf{t}}$ is the unitary tangential vector. The computation of the friction coefficient depends on the kind of rolling element [15, 16]. The contact between the rolling elements and the cage is also modelled by the Hertzian theory whereas the contact between the rings and the cage is simplified by considering that a nonlinear spring connects the centre of each part, taking into account the diameters of the parts. Regarding the restriction loads (force $\mathbf{f}_r$ and moment $\mathbf{m}_r$), they are caused because of the restrictions of the housing for the non-rotating ring, whereas they come from the loads applied to the shaft for the rotating ring.

Once the set of models for the parts, the contacts and the restrictions is obtained, the combination of the appropriate models leads to obtain the dynamics of bearings of any kind of rolling element and in any configuration, based on the reusability of models [12]. Moreover, as REBs work in different operating conditions regarding both the shaft speed and applied loads, the ability to reproduce either stationary or non-stationary operating conditions is introduced. This model is implemented by the use of Modelica® modelling language. The assembly of the models lead to the Newton-Euler equations for each part, which describe the dynamics of a REB with two rings, a cage and Z rolling elements:

$$m_i \cdot \mathbf{a}_i = m_i \cdot \mathbf{g} + \mathbf{f}_{c,i} + \mathbf{f}_{r,i} \tag{3}$$

$$m_o \cdot \mathbf{a}_o = m_o \cdot \mathbf{g} + \mathbf{f}_{c,o} + \mathbf{f}_{r,o} \tag{4}$$

$$m_{b_j} \cdot \mathbf{a}_{b_j} = m_{b_j} \cdot \mathbf{g} + \mathbf{f}_{c,b_j} \quad \forall j = 1, \ldots, Z \tag{5}$$

$$m_g \cdot \mathbf{a}_g = m_g \cdot \mathbf{g} + \mathbf{f}_{c,g} \tag{6}$$

$$\mathbf{I}_i \dot{\boldsymbol{\omega}}_i + \boldsymbol{\omega}_i \times \left(\mathbf{I}_i \boldsymbol{\omega}_i\right) = \mathbf{m}_{c,i} + \mathbf{m}_{r,i} \tag{7}$$

$$\mathbf{I}_o \dot{\boldsymbol{\omega}}_o + \boldsymbol{\omega}_o \times \left(\mathbf{I}_o \boldsymbol{\omega}_o\right) = \mathbf{m}_{c,o} + \mathbf{m}_{r,o} \tag{8}$$

$$\mathbf{I}_{b_j} \dot{\boldsymbol{\omega}}_{b_j} + \boldsymbol{\omega}_{b_j} \times \left(\mathbf{I}_{b_j} \boldsymbol{\omega}_{b_j}\right) = \mathbf{m}_{c,b_j} \quad \forall j = 1, \ldots, Z \tag{9}$$

$$\mathbf{I}_g \dot{\boldsymbol{\omega}}_g + \boldsymbol{\omega}_g \times \left(\mathbf{I}_g \boldsymbol{\omega}_g\right) = \mathbf{m}_{c,g} \tag{10}$$

where m is the mass of the body, $\mathbf{a}$ the acceleration of the gravity centre of the body, $\mathbf{g}$ the gravity vector, $\mathbf{f}_c$ the contact force vector, $\mathbf{f}_r$ the force vector due to the restrictions provided by the housing and the operating conditions, $\mathbf{I}$ the inertia tensor in the body-fixed system axes placed in the gravity centre of the body, $\dot{\boldsymbol{\omega}}$ the angular acceleration, $\boldsymbol{\omega}$ the angular velocity, $\mathbf{m}_c$ the contact moment vector and $\mathbf{m}_r$ the moment vector due to the restrictions provided by the housing and the operating conditions. Subscripts i, o, b and g stand for inner ring, outer ring, rolling element and cage, respectively. The vectors of Equations 3 to 6 are defined in the fixed reference system whereas the vectors of Equations 7 to 10 are defined in the body-fixed reference system.

3. EXPERIMENTAL TESTS

The validation of the model requires some knowledge about the real behaviour of a REB. Thus, the response of a REB is obtained by the use of a commercial test rig called Gearbox Prognostics Simulator, manufactured by SpectraQuest, Inc., shown in Figure 1a. It has the following components (from left to right): the driving motor, a monitored gearbox, another gearbox and a second motor, which is the responsible of applying torque load. The monitored gearbox has two reduction steps and six Rexnord ER16K REBs. Table 1 shows the dimensions and mechanical properties of this kind of REBs. In this study one of the REBs is tested in both healthy and damaged conditions. Specifically, the response one of the REBs of the intermediate shaft is analysed. Regarding damage conditions, damage with a diameter of 2 mm is seeded in the outer ring.

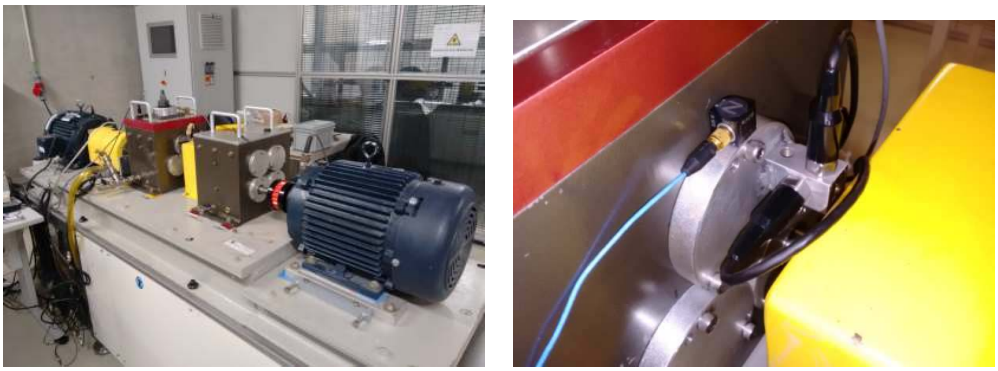

(a) (b)

Figure 1: Experimental equipment: (a) test rig, (b) accelerometers on the housing

Table 1: Dimensions and mechanical properties of the Rexnord ER16K

Parameter	**Value**
Number of balls, Z	9
Ball diameter, D_w	7.94 mm
Inner race diameter, d_i	31.38 mm
Outer race diameter, d_o	47.26 mm
Pitch diameter, d_m	39.32 mm
Race groove radius, r	4.1 mm

Tests in different operating conditions have been done. The speed of the drive motor is set to different constant values: 250 rpm, 500 rpm, 1000 rpm and 1500 rpm. As the monitored REB is placed in the intermediate shaft, the ratio of the first step has to be taken into account. As this value is equal to 5/2, the speeds at which the REB is operating are 100 rpm, 200 rpm, 400 rpm and 600 rpm, respectively. The length of each test has been defined as the one that the axis of the REB needs to take 60 turns. Thus, the tests have a length of 36 s, 18 s, 9 s and 6 s, respectively. Moreover, a test in non-stationary operating conditions has been done, in such a way that the speed of the shaft increases linearly from 600 rpm to 1000 rpm in 9.6 s. This leads to a speed change from 240 rpm to 400 rpm in the tested REB.

The vibratory excitation of the REB is measured by means of three accelerometers, as shown in Figure 1b. In detail, the acquisition system is composed by a triaxial PCB 356A17 accelerometer placed on the housing of the REB and two IPC 608A11 uniaxial accelerometers. The sampling frequency is defined as 10240 Hz for the triaxial accelerometer and 50000 Hz for the two uniaxial accelerometers.

4. EXPERIMENTAL VALIDATION OF THE MODEL

Simulations describing the scenarios described in Section 3 are carried out by the use of the physics-based model cited in Section 2. Thus, simulations involving five shaft speeds (the aforementioned four constant values and the transient speed) and two bearing conditions (healthy state and a case with a damaged outer ring) are obtained. These simulations are done by using a time step of 1 ms and a tolerance of 10^{-4}. The acceleration signals are extracted from each of the simulations to be analysed in this section.

The validation of the model is based on the analysis of the characteristic frequencies. In the case of a damaged outer ring, excitation in the ball pass frequency of outer ring (BPFO) and its harmonics is expected [17]. BPFO is calculated as

$$BPFO = Z \cdot \frac{n}{2} \cdot \left(1 - \frac{D_w}{d_m} \cdot \cos\phi\right) \tag{11}$$

where n is the shaft speed and ϕ is the contact angle. As only radial load is applied to the shaft, it can be assumed that the value of the contact angle ϕ is zero.

Figures 2 to 5 present the frequency spectrum of the acceleration signals obtained by the simulations and the tests in the four constant shaft speeds, and Table 2 shows the characteristic frequency values

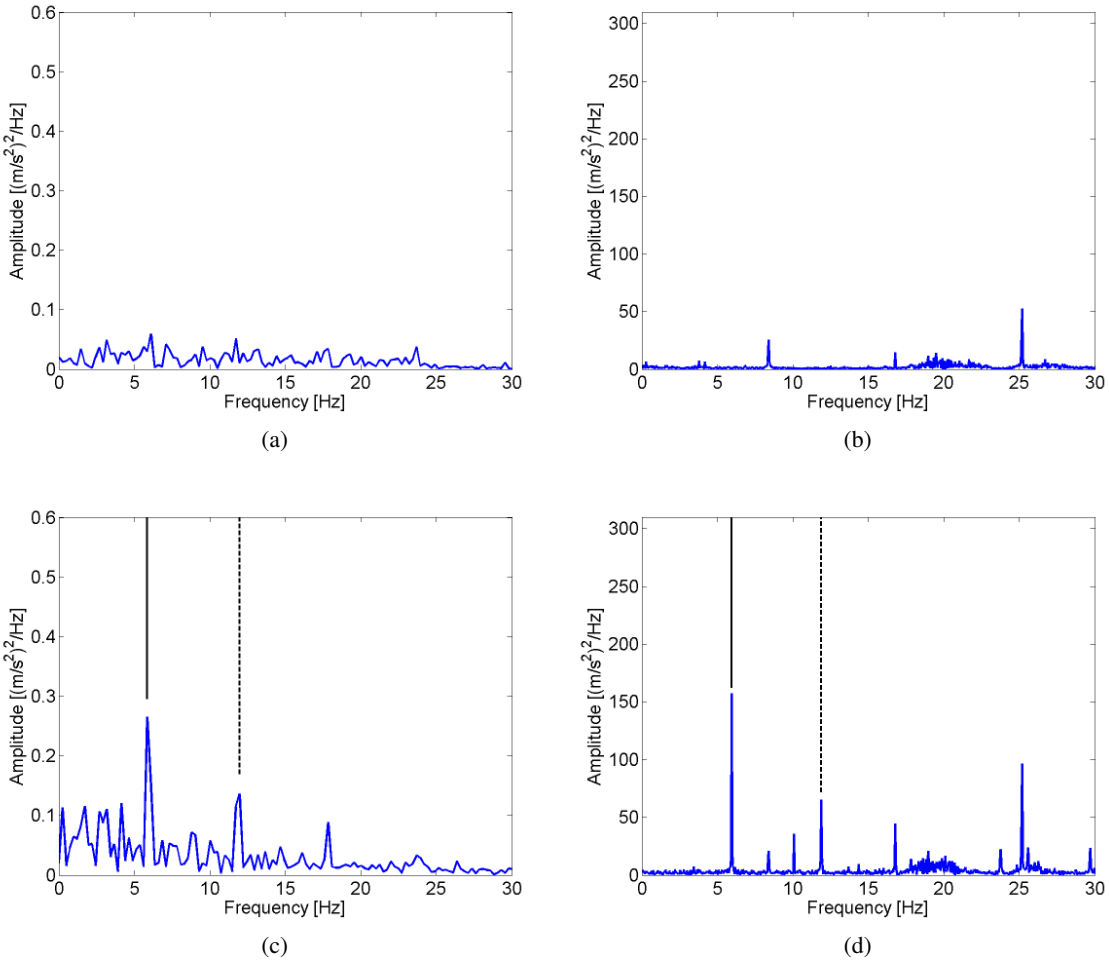

Figure 2: Frequency analysis of the model and the tests at 100 rpm: (a) model in healthy case, (b) test in healthy case, (c) model in damaged case, (d) test in damaged case

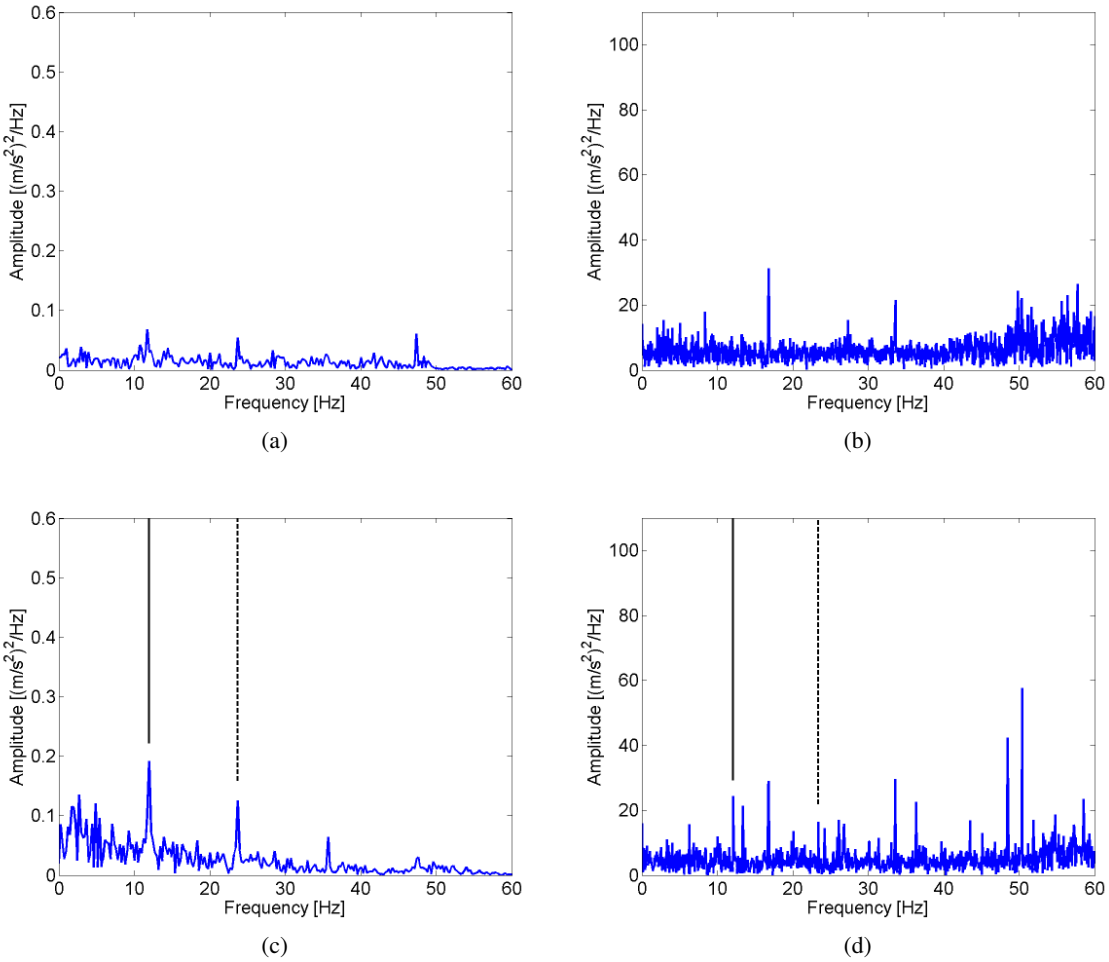

Figure 3: Frequency analysis of the model and the tests at 200 rpm: (a) model in healthy case, (b) test in healthy case, (c) model in damaged case, (d) test in damaged case

Table 2: Comparison of the characteristic frequencies obtained by the model, the experiments and the theoretical results (values between parentheses show the differences of the model results with respect to the experimental and the theoretical results)

Speed	**Frequency**	**Proposed model**	**Experimental**	**Theoretical**
250 rpm	BPFO	5.86 Hz	5.93 Hz (-1.25 %)	5.95 Hz (-1.59 %)
250 rpm	2·BPFO	11.96 Hz	11.87 Hz (0.81 %)	11.91 Hz (0.46 %)
500 rpm	BPFO	11.96 Hz	12.11 Hz (-1.22 %)	11.91 Hz (0.46 %)
500 rpm	2·BPFO	23.68 Hz	23.39 Hz (1.25 %)	23.82 Hz (-0.56 %)
1000 rpm	BPFO	23.68 Hz	24.25 Hz (-2.34 %)	23.82 Hz (-0.56 %)
1000 rpm	2·BPFO	47.61 Hz	48.5 Hz (-1.84 %)	47.63 Hz (-0.05 %)
1500 rpm	BPFO	35.64 Hz	36.2 Hz (-1.53 %)	35.72 Hz (-0.22 %)
1500 rpm	2·BPFO	71.29 Hz	72 Hz (-0.99 %)	71.45 Hz (-0.22 %)

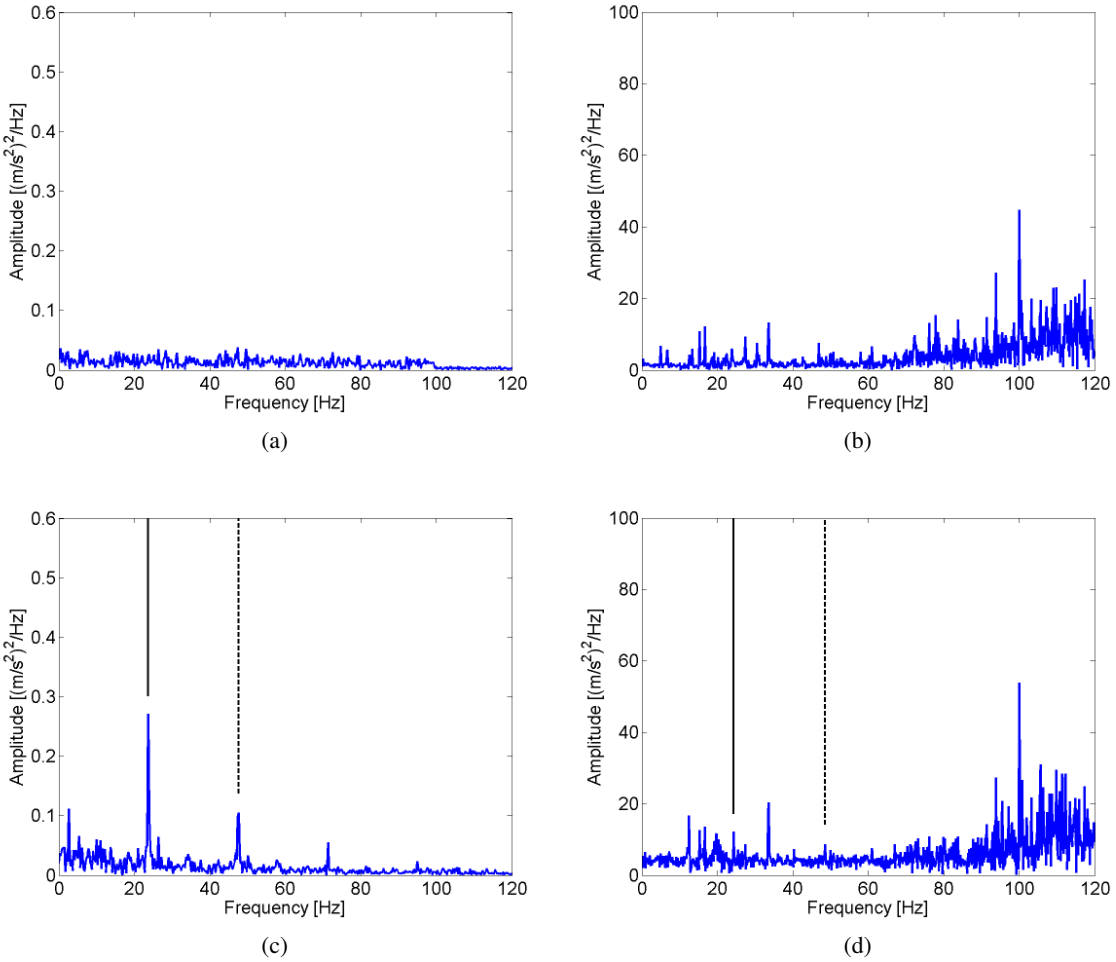

Figure 4: Frequency analysis of the model and the tests at 400 rpm: (a) model in healthy case, (b) test in healthy case, (c) model in damaged case, (d) test in damaged case

related to the damaged cases. The response of both healthy and damaged conditions for both simulation and experimental results can be seen in each figure. Regarding the results obtained by the model, the ones related to the healthy state have an almost flat response whereas the ones related to the damage state show clearly excitation in the BPFO and its harmonics. The spectral content of the experimental results is more complex due to the fact that the vibration response of other components of the test rig is coupled to the one related to the monitored REB. Thus, peaks related to the speeds of the three shafts of the gearbox in which the monitored REB is placed as well as their harmonics can be found. The analysis of the response of the damaged cases shows that the BPFO and its first harmonic can be easily identified in both the simulation and experimental results. Higher harmonics, such as the second one, can still be found in the simulation results, whereas there are more difficulties to identify them in the experimental results.

The characteristic frequency values presented in Table 2 show that the response of the model is close to both the experimental results and the theoretical results given by Equation 11. In fact, differences lower than 1.6 % can be found when compared the simulation results to the theoretical results and differences lower than 2.35 % when compared them to the experimental results for any of the operating conditions, as it is shown in Table 2.

Concerning non-stationary operating conditions, results for the case in which the shaft speed varies

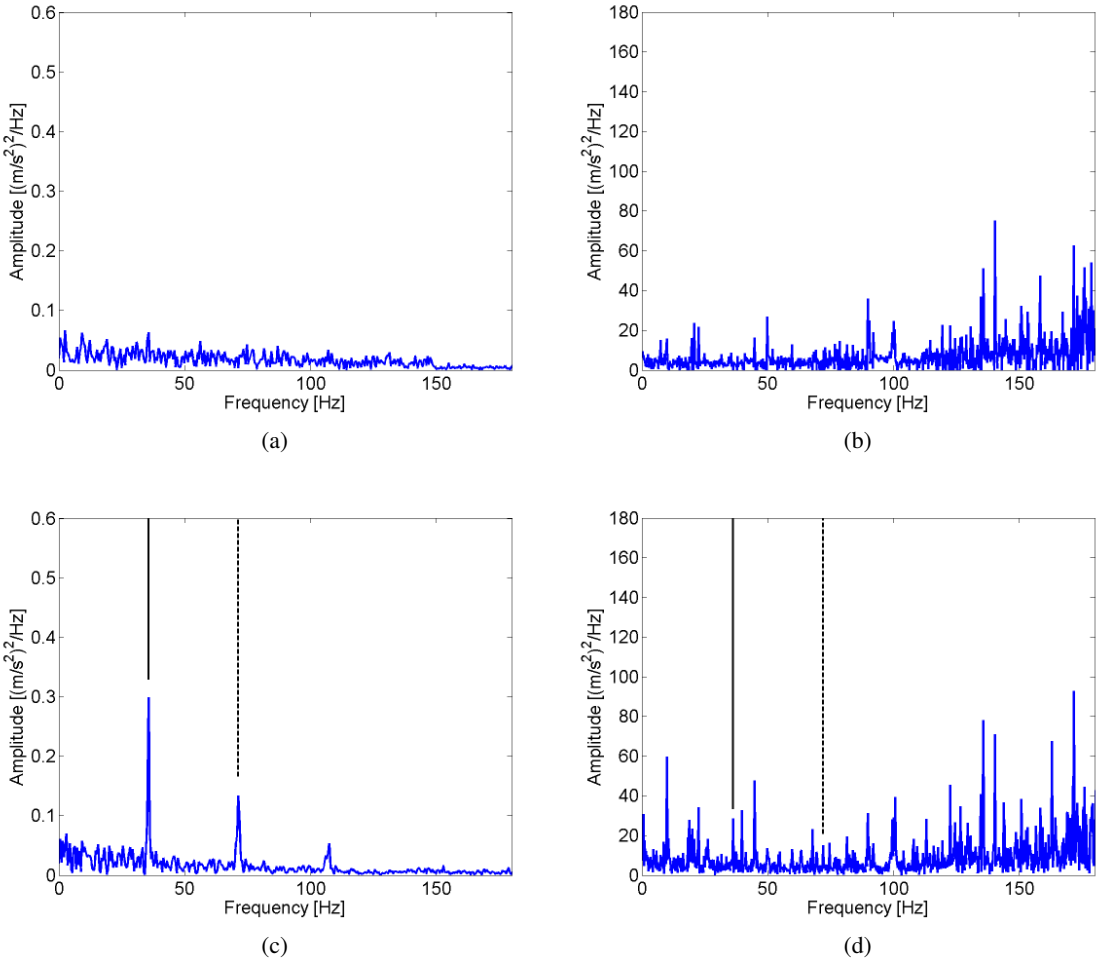

Figure 5: Frequency analysis of the model and the tests at 600 rpm: (a) model in healthy case, (b) test in healthy case, (c) model in damaged case, (d) test in damaged case

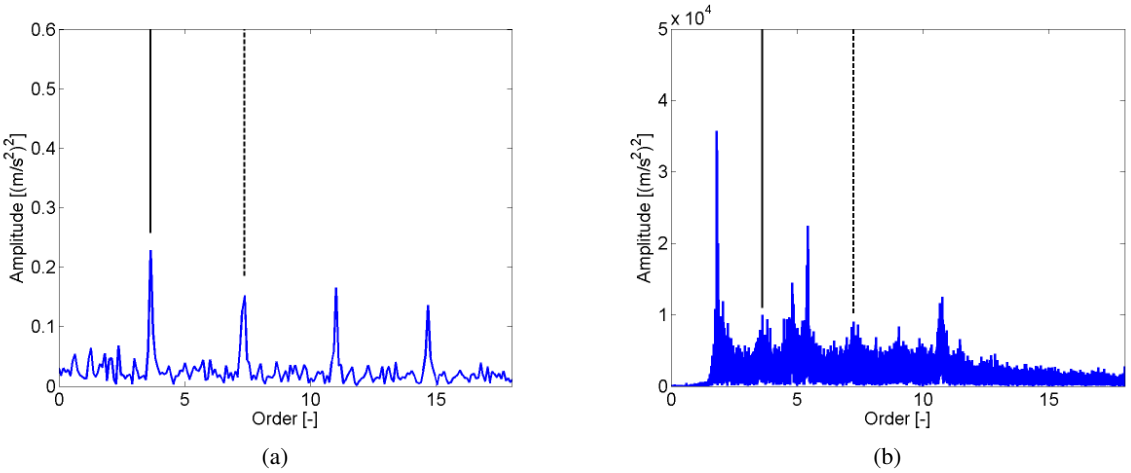

Figure 6: Order analysis of the model and the tests with variable speed: (a) model in damaged case, (b) test in damaged case

linearly with time from 240 rpm to 400 rpm are shown in Figure 6. In that case order analysis is performed, in such a way that the identification of the ball pass order of outer ring (BPOO) is wanted instead of the BPFO. Thus, a similar behaviour is obtained from the model and the experimental results as the BPOO and its two harmonics are found whereas only the BPOO and its first harmonic are identified in the tests. The values of these last orders are presented in Table 3, and differences lower than 3.25 % when compared to the theoretical results and differences lower than 2 % when compared to the experimental results are found. As these results are accurate enough for this application, the validation of the model is proved.

Table 3: Comparison of the characteristic orders obtained by the model, the experiments and the theoretical results (values between parentheses show the differences of the model results with respect to the experimental and the theoretical results)

Order	**Proposed model**	**Experimental**	**Theoretical**
BPOO	3.64	3.62 (0.51 %)	3.57 (1.97 %)
2·BPOO	7.38	7.23 (1.97 %)	7.14 (3.24 %)

5. CONCLUSIONS

In the last decades, the use of physics-based modelling has been proved to be a useful tool for getting knowledge about a system and obtaining valuable information regarding its healthy or damaged condition. Nevertheless, it should be highlighted that the application of this kind of modelling to complex systems has some limitations, specially concerning the interactions between the elements. Therefore, its applicability is mainly limited to the component level.

In the field of rotary machinery, the use of physics-based modelling applied to REBs has been widely extended as they are key parts of this kind of machines. In this work the validation process of a model developed by the authors is presented. This model is based on a multi-body approach and its aim is to represent the behaviour of any kind of rolling element, bearing configuration, operating condition and bearing condition. In this case it is adapted for a single-row deep-groove ball bearing, as it is the kind of bearing that has been tested. Experimental tests have been done in a commercial test rig in different speeds and using a healthy and a damaged bearing.

The acceleration signals provided by the simulations and the ones acquired by the accelerometers placed on the housing of the monitored REB are analysed. The presence of excitation near the BPFO and its harmonics is analysed for both simulation and experimental results. An agreement between these results as well as between the simulation and the theoretical results is found, with differences lower than 2% and 3.25%, respectively. Thus, it can be concluded that the model gives an accurate representation of the behaviour of this kind of REBs in a range of operating conditions, in such a way that the model is validated.

ACKNOWLEDGEMENTS

This study is partially funded by the Ministry of Economy and Competitiveness of the Spanish Government under the Retos-Colaboración Program (LEMA project, RTC-2014-1768-4). Any opinions, findings and conclusions expressed in this article are those of the authors and do not necessarily reflect the views of funding agencies. The authors would also like to thank Fundación de Centros Tecnológicos - Iñaki Goenaga.

REFERENCES

[1] S. Singh, C. Q. Howard, and C. H. Hansen. An extensive review of vibration modelling of rolling element bearings with localised and extended defects. *Journal of Sound and Vibration*, 357:300–330, November 2015.

[2] X. Yuan, Y.-S. Zhu, and Y.-Yun Zhang. Multi-body vibration modelling of ball bearing-rotor system considering single and compound multi-defects. *Proceedings of the Institution of Mechanical Engineers, Part K: Journal of Multi-body Dynamics*, 228(2):199–212, June 2014.

[3] L. Niu, H. Cao, Z. He, and Y. Li. A systematic study of ball passing frequencies based on dynamic modeling of rolling ball bearings with localized surface defects. *Journal of Sound and Vibration*, 357:207–232, November 2015.

[4] G. Kogan, R. Klein, A. Kushnirsky, and J. Bortman. Toward a 3d dynamic model of a faulty duplex ball bearing. *Mechanical Systems and Signal Processing*, 54-55:243–258, March 2015.

[5] J. Sopanen and A. Mikkola. Dynamic model of a deep-groove ball bearing including localized and distributed defects. Part 1: Theory. *Proceedings of the Institution of Mechanical Engineers, Part K: Journal of Multi-body Dynamics*, 217(3):201–211, September 2003.

[6] M. Nakhaeinejad and M. D. Bryant. Dynamic modeling of rolling element bearings with surface contact defects using bond graphs. *Journal of Tribology*, 133(1):011102, January 2011.

[7] V. N. Patel, N. Tandon, and R. K. Pandey. A dynamic model for vibration studies of deep groove ball bearings considering single and multiple defects in races. *Journal of Tribology*, 132(4):041101, October 2010.

[8] S. Sassi, B. Badri, and M. Thomas. A numerical model to predict damaged bearing vibrations. *Journal of Vibration and Control*, 13(11):1603–1628, November 2007.

[9] H. Arslan and N. Aktrk. An investigation of rolling element vibrations caused by local defects. *Journal of Tribology*, 130(4):041101, October 2008.

[10] D. Petersen, C. Howard, N. Sawalhi, A. M. Ahmadi, and S. Singh. Analysis of bearing stiffness variations, contact forces and vibrations in radially loaded double row rolling element bearings with raceway defects. *Mechanical Systems and Signal Processing*, 50-51:139–160, January 2015.

[11] A. Choudhury and N. Tandon. Vibration response of rolling element bearings in a rotor bearing system to a local defect under radial load. *Journal of Tribology*, 128(2):252–261, April 2006.

[12] U. Leturiondo, M. Mishra, O. Salgado, and D. Galar. Nonlinear response of rolling element bearings with local defects. In *Proceedings of The Eleventh International Conference on Condition Monitoring and Machinery Failure Prevention Technologies*, Manchester, United Kingdom, June 2014.

[13] T. A. Harris and M. N. Kotzalas. *Essential concepts of bearing technology*. Rolling bearing analysis. Taylor & Francis, New York, 5 edition, 2006.

[14] P. Flores, J. Ambrósio, J. C. Pimenta Claro, and H. M. Lankarani. *Kinematics and dynamics of multibody systems with imperfect joints*. Springer Berlin Heidelberg, 2008.

[15] H. Spikes. Basics of ehl for practical application. *Lubrication Science*, 27(1):45–67, January 2015.

[16] P. K. Gupta. *Advanced dynamics of rolling elements*. Springer New York, 1 edition, 1984.

[17] Wade A. Smith and Robert B. Randall. Rolling element bearing diagnostics using the case western reserve university data: A benchmark study. *Mechanical Systems and Signal Processing*, 64-65:100–131, December 2015.